Molecular Pharmacology Fast Forward. Published on February 16, 2007 as doi:10.1124/mol.106.033233
This article has not been copyedited and formatted. The final version may differ from this version.

Analogs of Methyllycaconitine as Novel Noncompetitive Inhibitors of Nicotinic Receptors: Pharmacological Characterization, Computational Modeling, and Pharmacophore Development

Dennis B. McKay, Cheng Chang, Tatiana F. González, Susan B. McKay, Raed A. El-Hajj, Darrell L. Bryant, Michael X. Zhu, Peter W. Swaan, Kristjan M. Arason, Aravinda B. Pulipaka, Crina M. Orac, and Stephen C. Bergmeier

Division of Pharmacology, College of Pharmacy, The Ohio State University, Columbus, OH (DBM, TFG, SBM, RAE, DLB); Department of Pharmaceutical Sciences, School of Pharmacy, University of Maryland, Baltimore, MD (CC, PWS); Department of Neuroscience, College of Medicine, The Ohio State University, Columbus, OH (MXZ); Department of Chemistry and Biochemistry, Ohio University, Athens, OH (KMA, APB, CMO, SCB)

Molecular Pharmacology Fast Forward. Published on February 16, 2007 as DOI: 10.1124/mol.106.033233
This article has not been copyedited and formatted. The final version may differ from this version.

RUNNING TITLE PAGE

RUNNING TITLE: Computational Modeling and Pharmacophore Development

CORRESPONDING AUTHOR: Dennis B. McKay, Ph.D.

Division of Pharmacology

The Ohio State University

College of Pharmacy

500 West 12th Avenue

Columbus, Ohio 43210

Telephone #: (614) 292-3771

Telefax #: (614) 292-9083

email: mckay.2@osu.edu

Text pages: 34
Tables: 5
Figures: 9
References: 29
Word count: Abstract: 250
Introduction: 531
Discussion: 1230

List of nonstandard abbreviations: neuronal nicotinic acetylcholine receptors (nAChRs), methyllycaconitine (MLA), quantitative structure-activity relationship (QSAR), comparative molecular field analysis (CoMFA), comparative molecular similarity index analysis (CoMSIA), partial least square (PLS), genetic algorithm similarity program (GASP), predictive error sum of squares (PRESS), hydrogen-bond acceptor (HBA)

Molecular Pharmacology Fast Forward. Published on February 16, 2007 as DOI: 10.1124/mol.106.033233
This article has not been copyedited and formatted. The final version may differ from this version.

ABSTRACT

As a novel approach to drug discovery involving neuronal nicotinic acetylcholine receptors (nAChRs), our laboratory is targeting non-agonist binding sites (i.e., noncompetitive binding sites, negative allosteric binding sites) located on nAChRs. Cultured bovine adrenal cells were used as neuronal models to investigate interactions of 67 analogs of methyllycaconitine (MLA) on native $\alpha3\beta4$* nAChRs. The availability of large numbers of structurally-related molecules presents a unique opportunity for the development of pharmacophore models for noncompetitive binding sites. Our MLA analogs inhibited nicotine-mediated functional activation of both native and recombinant $\alpha3\beta4$* nAChRs with a wide range of IC_{50} values (0.9 to 115 μM). These analogs had little or no inhibitory effects on agonist binding to native or recombinant nAChRs, supporting noncompetitive inhibitory activity. Based on these data, two highly predictive 3D-QSAR (CoMFA and CoMSIA) models were generated. These computational models were successfully validated and provided insights into the molecular interactions of MLA analogs with nAChRs. Additionally, a pharmacophore model was constructed to analyze and visualize the binding requirements to the analog binding site. The pharmacophore model was subsequently applied to search structurally diverse molecular databases in order to prospectively identify novel inhibitors. The rapid identification of 8 molecules from database mining and our successful demonstration of in vitro inhibitory activity support the utility of these computational models as novel tools for the efficient retrieval of inhibitors. These results demonstrate the effectiveness of computational modeling and pharmacophore development, which may lead to the identification of new therapeutic drugs that target novel sites on nAChRs.

Molecular Pharmacology Fast Forward. Published on February 16, 2007 as DOI: 10.1124/mol.106.033233
This article has not been copyedited and formatted. The final version may differ from this version.

The physiological roles of neuronal nicotinic acetylcholine receptors (nAChRs) in synaptic release of acetylcholine and their involvement in the modulation of other important neurotransmitters such as norepinephrine, serotonin, gamma aminobutyric acid (GABA), glutamate, and dopamine make nAChRs prime targets for therapeutic interventions. In addition, nAChRs have been linked to pain, epilepsy, and many neurodegenerative diseases, such as Alzheimer's disease and Parkinson's disease, and psychiatric disorders, such as depression and schizophrenia. The development of new drugs to target these receptors has been slow for several reasons: 1) multiple subtypes of nAChRs are expressed in the central and peripheral nervous systems, 2) few drugs are available that selectively target nAChR subtypes, and 3), information on the physiological roles of specific nAChR subtypes is limited. A key approach to provide a better understanding of physiological processes and pathophysiological conditions involving nAChRs is the identification and development of small molecules that selectively interact with specific nAChR subtypes.

A variety of agents have been found in nature that interact with nAChRs (Daly, 2005), some of which are used to pharmacologically differentiate nAChR subtypes, including snake venom neurotoxins (e.g., Luetje *et al.*, 1990) and marine snail conotoxins (e.g., Livett *et al.*, 2004). However, a problem associated with the therapeutic usefulness of these molecules is that they are proteins. The plant alkaloid, methyllycaconitine (MLA) is a hexacyclic norditerpenoid with a well-documented high affinity, competitive antagonism for α7 nAChRs (Ward *et al.*, 1990). However, MLA also acts as a competitive antagonist on other nAChR subtypes, including α3β4 nAChRs (Bryant *et al.*, 2002; Free *et al.*, 2002; Free *et al.*, 2003) and α4β2 nAChRs (Yum *et al.*,

1996), albeit with lower affinity. This activity of MLA on multiple neuronal nAChR subtypes suggests that MLA analogs could be used to elucidate structural determinants important for activity on specific nAChR subtypes.

Taking this approach, our laboratory (Bergmeier *et al.*, 1999; Bryant *et al.*, 2002; Bergmeier *et al.*, 2004) and others (e.g., Goodall *et al.*, 2005), have synthesized analogs of MLA. Our laboratory has reported that these analogs appear to act as noncompetitive inhibitors of $\alpha3\beta4^*$ nAChRs, based on their ability to inhibit nAChR-mediated neurosecretion without inhibition of agonist binding to nAChRs (Bergmeier *et al.*, 1999; Bryant *et al.*, 2002; Bergmeier *et al.*, 2004). In addition, these analogs had no effects on agonist binding to $\alpha4\beta2$ and $\alpha7$ nAChRs (Bergmeier *et al.*, 1999; Bryant *et al.*, 2002; Bergmeier *et al.*, 2004). Similar findings have recently been reported by Barker and associates with a tricyclic analog of MLA (Barker *et al.*, 2005). We now report on the pharmacological activities of 67 MLA analogs on functional activation of native and recombinant nicotinic receptors. Our hypotheses are that these pharmacological studies, using such large numbers of structurally similar compounds, can be used to generate predictive 3D-QSAR models and to calculate a pharmacophore model. Our goal, more importantly, is to apply the pharmacophore model to search structurally diverse molecular databases in order to prospectively identify novel nAChR inhibitors. The successful identification of novel molecules using computational models and the demonstration of their *in vitro* activity will be valuable tools for the efficient retrieval of novel or hitherto unrecognized nAChR inhibitors, potentially leading to subtype-selective nAChR antagonists.

Molecular Pharmacology Fast Forward. Published on February 16, 2007 as DOI: 10.1124/mol.106.033233
This article has not been copyedited and formatted. The final version may differ from this version.

MATERIALS AND METHODS

Materials. (-)Nicotine hydrogen tartrate, polyethyleneimine and components of N2+ media were obtained from the Sigma Chemical Company (St. Louis, MO). Dulbecco's Modified Eagle Medium (DMEM), DMEM/F12 (used in N2+ medium) and Minimum Essential Medium (MEM), as well as the antibiotics and L-glutamine were obtained from Invitrogen Corporation (Grand Island, NY). Fluo-4-acetoxymethylester (Fluo-4-AM), probenecid, and pluronic F-127 were obtained from Molecular Probes (Eugene, OR). (+/-)[5,6-bicycloheptyl-^{3}H]-Epibatidine (specific activity, 55.5 Ci/mmol) and DL-[7-^{3}H(N)]-norepinephrine hydrochloride (specific activity, 10-15 Ci/mmol) were purchased from PerkinElmer Life and Analytical Sciences (Boston, MA). Whatman GF/B filters were purchased from Brandel Laboratories, Inc. (Gaithersburg, MD). Bovine adrenal glands were purchased from the Herman Falter Packing Company (Columbus, OH). MLA analogs (Figures 1 and 9) were in general prepared by reaction of hydroxymethyl piperidine with the appropriate alkyl halide to provide the N-alkyl hydroxymethyl piperidine. This compound was then coupled to the appropriate carboxylic acid to provide the target MLA analog (Bergmeier *et al.*, 2004). All compounds were pure as shown by ^{1}H NMR, ^{13}C NMR, and HRMS.

Neurosecretion Studies. Bovine adrenal chromaffin cells were dissociated from intact glands and placed into culture, as previously described by our laboratory (Maurer and McKay, 1994). A [^{3}H]norepinephrine assay was used to monitor neurosecretion from cultured cells (Maurer and McKay, 1994). Cells were typically used experimentally 4-7 days after isolation. Cells were pretreated for 15 min with the analogs prior to stimulation with nicotine (10 µM) in the continued presence of the analog. Due to

Molecular Pharmacology Fast Forward. Published on February 16, 2007 as DOI: 10.1124/mol.106.033233
This article has not been copyedited and formatted. The final version may differ from this version.

solubility problems, IC_{50} values of a few analogs (APB 1, 4, and 11) could not be precisely determined; values of 10 µM for these analogs were used for modeling purposes. Results were calculated from the number of observations (n) performed in duplicate or triplicate. IC_{50} values were obtained by averaging values generated from nonlinear regression analyses (Prizm, GraphPad, San Diego, CA) of individual concentration-response curves. Concentration-response data are expressed as geometric means (95% confidence limits). Linear regression analyses were performed using Prizm with the level of significance set at $p<0.05$.

[^{3}H]Epibatidine Binding to Native and Recombinant α3β4 nAChRs.

Membrane preparations from bovine adrenal medullary tissues were prepared and agonist binding experiments were performed as previously described by our laboratory (Free *et al.*, 2002). Briefly, adrenal membranes were incubated at room temperature for 60 min in 500 µl of assay/rinse buffer (120 mM Na2Cl2, 5 mM KCl, 8 mM Na2HPO4, 0.1 mM phenylmethylsulfonyl fluoride, 5 mM iodoacetamide, 2 mM EDTA, 2 mM EGTA, 5 mM HEPES (pH 7.4) containing 1 nM [^{3}H]epibatidine. α-bungarotoxin (αBGT) (1 µM) was added to the buffer to eliminate potential radiolabeled ligand binding to αBGT binding sites. For the analog competition binding studies, membranes were incubated without (control) or with 10 µM concentrations of the analogs. Nonspecific binding was determined in the presence of 300 µM nicotine (typically 5-10% of total binding). A HEK 293 cell line stably expressing bovine α3β4 nAChRs (BMα3β4 cells) developed by our laboratory was used as a rich source of recombinant bovine adrenal α3β4 nAChRs (Free *et al.*, 2002). nAChR binding experiments using BMα3β4 cell membrane preparations were performed by modification of procedures previously described by our

Molecular Pharmacology Fast Forward. Published on February 16, 2007 as DOI: 10.1124/mol.106.033233
This article has not been copyedited and formatted. The final version may differ from this version.

laboratory (Free *et al.*, 2003). Briefly, HEK cell membranes were prepared using MPER™, according to manufacturer's instructions and with the addition of a protease inhibitor cocktail (Roche). Membranes were incubated at room temperature for 60 min in a binding/rinse buffer containing 1 nM [^{3}H]epibatidine. For the analog competition binding studies, membranes were incubated without (control) or with 10 µM concentrations of the analogs. Nonspecific binding was determined in the presence of 300 µM nicotine. Specific binding was determined by subtracting nonspecific binding (typically 1-2% of total binding) from total binding.

Measurement of Intracellular Calcium Using HEK 293 Cells Stably Expressing Recombinant nAChRs. For theses studies BMα3β4 cells that express bovine adrenal α3β4 nAChRs and KXα3β4R cells (Xiao *et al.*, 1998) that express rat α3β4 nAChRs were used. Cells were plated on poly-d-lysine coated 96-well plates at a density of 1.2-1.5 x 10^5 cells per well and incubated at 37ºC in 5% CO_2, using minimum essential medium supplemented with 10% fetal bovine serum, 10 mM L-glutamine, 0.7 mg/ml G418, 100 units/ml penicillin, and 100 µg/ml streptomycin. Forty-eight hours after plating, cells were washed with HBK buffer (155 mM NaCl, 4.6 mM KCl, 1.2 mM $MgSO_4$, 1.8 mM $CaCl_2$, 6 mM glucose and 20 mM HEPES, pH 7.4) for KXα3β4R cells or with HBK buffer with 20 mM $CaCl_2$ for BMα3β4 cells and loaded with 2 µM fluo-4-AM in the presence of 2.5 mM probenecid and 0.05% pluronic F-127 for 1 hr at 24ºC and protected from light. At the end of the incubation period, the cells were washed once more and basal fluorescence was measured using a fluid handling integrated fluorescence plate reader (Flex Station, Molecular Devices, Sunnyvale, CA). Responses after addition of agonists were recorded for 20 seconds. When analogs were tested,

Molecular Pharmacology Fast Forward. Published on February 16, 2007 as DOI: 10.1124/mol.106.033233
This article has not been copyedited and formatted. The final version may differ from this version.

cells were preincubated for 40 seconds prior to stimulation in the continued presence of the analog. Probenecid (2.5 mM) was included in all of the solutions once the cells were loaded to prevent the leakage of fluo-4 from the cell. The fluo-4 fluorescence was read at an excitation of 494 nm and an emission of 520 nm from the bottom of the plate.

Molecular Modeling and Structure Building. The computational molecular modeling studies were carried out using a Silicon Graphics (Palo Alto, CA) Octane workstation with the IRIX 6.5 operating system running the SYBYL software suite version 6.9 (Tripos Inc., St. Louis, MO, USA). The molecular structures of the analogs were built using standard bond distances and bond angles with the sketch module of SYBYL. All molecules were charged according to physiological conditions. Partial atomic charges were then calculated using the Gasteiger-Marsili method. The energy minimizations were performed using Tripos force field with a distance-dependent dielectric coefficient and the Powell conjugate gradient algorithm with an energy change convergence criterion of 0.001 kcal/mol.

GASP. GASP (Genetic Algorithm Similarity Program) is a genetic algorithm, developed for the perception of pharmacophore models through superimposition of flexible molecules (Jones *et al.*, 1995). When aligning a set of molecules, GASP attempts to optimize the orientation and conformation of molecules at the same time by quickly and efficiently fitting them to similarity constraints. One major limitation of GASP is that each run can only align four to five molecules depending on the molecular complexity. In order to align all 67 compounds using GASP, they were separated into 19 groups of either 4 or 5 compounds, each containing the model compound IB 12. Compounds in each group were aligned to IB 12 using GASP. All aligned structures

Molecular Pharmacology Fast Forward. Published on February 16, 2007 as DOI: 10.1124/mol.106.033233
This article has not been copyedited and formatted. The final version may differ from this version.

from different groups were subsequently merged together and used as input for later CoMFA and CoMSIA studies. When generating the alignment, to broaden the diversity of conformations that were considered, the "population size" was increased to 125 and the "allele mutate weight" to 96. With increased population size and mutation rates, conformations with more diversity were generated. To avoid possible problems with convergence because of the increased mutation rate, the convergence criteria were loosened by increasing the "fitness increment" to 0.02. Ten alignments were generated and the best model was selected through visual inspection based on chemical intuition.

In order to generate a pharmacophore model for this set of analogs, four representative potent analogs (IB 12, IB 9, PPB 3, PPB 13) were selected. The most potent, IB 12, was chosen as the template for alignment. The same GASP settings were maintained for pharmacophore generation.

CoMFA. SYBYL/CoMFA is a successful implementation of 3D-QSAR technique that explains the gradual changes in observed biological properties by evaluating the electrostatic (Coulombic interactions) and steric (van der Waals interactions) fields at regularly spaced grid points surrounding a set of mutually aligned ligands (Cramer *et al.*, 1988). The interaction fields were calculated using an sp^3 hybridized carbon probe atom (+1 charge at 1.52 Å van der Waals radius) on a 2.0 Å spaced lattice, which extends beyond the dimensions of each structure by 4.0 Å in all directions. Due to the steep steric and electrostatic potential functions when the probe atom is placed close to the molecule van der Waals surface, a cutoff value of 30 kcal/mol was set to ensure that no extreme energy terms will distort the final model. In order to reduce chance correlation and effectively correlate the huge number of field descriptors with relatively few

Molecular Pharmacology Fast Forward. Published on February 16, 2007 as DOI: 10.1124/mol.106.033233
This article has not been copyedited and formatted. The final version may differ from this version.

biological activities, the statistical algorithm, Partial Least Square (PLS), was adopted (Clark and Cramer III, 1993). The indicator fields (Kroemer and Hecht, 1995) and hydrogen bond fields (Bohacek and McMartin, 1992) generated by the "advanced CoMFA" module were also included in the analysis. Among the 67 tested analogs, 6 were randomly selected as test set and the rest (61) were used as a training set for model generation. CoMFA descriptors were used as independent variables, whereas the dependent variable (biological descriptor) used in these studies was the negative logarithm of the analog IC_{50} values (-Log IC_{50}) for their inhibition of $\alpha 3\beta 4$ nAChR-mediated bovine adrenal neurosecretion. The predictive value of the models was initially evaluated using Leave-One-Out (LOO) cross-validation. The cross-validated coefficient, q^2, is calculated as follows:

$$q^2 = 1 - \frac{\sum_{Y} \left(Y_{predicted} - Y_{observed}\right)^2}{\sum_{Y} \left(Y_{observed} - Y_{mean}\right)^2} \qquad (1)$$

where $Y_{predicted}$, $Y_{observed}$, and Y_{mean} are the predicted, observed and mean values of the target property (-Log IC_{50}), respectively. $\Sigma(Y_{predicted}-Y_{observed})^2$ is the predictive error sum of squares (PRESS). The standard error of the cross-validated predictions is known as "press", and the root mean square of the conventional (noncross-validated) predictions is labeled "s". The model with the optimum number of principal components, corresponding to the lowest PRESS value, was selected for deriving the final PLS regression models (Table 2). Contour of std*coefficients enclosing the most significant value were plotted (Figure 3).

CoMSIA. SYBYL/CoMSIA is an extension of CoMFA methodology developed by Klebe and colleagues (Klebe *et al.*, 1994). They differ only in the implementation of the

interaction fields. Instead of using Lennard-Jones potential (steric fields) and Coulombic potential (electrostatic fields), CoMSIA uses a Gaussian type function to avoid the extreme values generated by the two functions, thus eliminating the requirement of setting a cutoff value in field generation process. The Gaussian function also results in smoother, less fragmented surfaces in the final model representation. Five physicochemical properties (steric, electrostatic, hydrophobic, hydrogen bond donor, and hydrogen bond acceptor) were evaluated using a positively charged sp^3 hybridized carbon probe atom. The same set of training set and test set compounds with identical alignment from the CoMFA study were used for the generation and evaluation of the CoMSIA model. A field contour was similarly plotted (Figure 4).

UNITY. UNITY (Tripos Inc., St. Louis, MO, USA) is a database screening and analyzing tool that is capable of 2D and 3D searches. It performs flexible 3D database searching by implementing the directed tweak technique (Hurst, 1994). A UNITY query was prepared by extracting the chemical features as well as the feature constraints from the previously generated GASP pharmacophore model. The query was subsequently modified to optimize both specificity and selectivity. Flexible searches of 445742 compounds from both Chembridge (241903 compounds) and Spec (203839 compounds) databases were performed. The distance constraints tolerance was increased from the default 0.1A to 0.5A to increase the chance of retrieving more diversified hit compounds.

Molecular Pharmacology Fast Forward. Published on February 16, 2007 as DOI: 10.1124/mol.106.033233
This article has not been copyedited and formatted. The final version may differ from this version.

RESULTS

Our laboratory has synthesized a library of analogs of MLA. Although MLA itself is a competitive inhibitor of both native (Free *et al.*, 2002) and recombinant (Free *et al.*, 2003) $\alpha 3\beta 4$ nAChRs, our data support the inhibitory activity of several MLA analogs as noncompetitive in nature (Bergmeier *et al.*, 1999; Bryant *et al.*, 2002; Bergmeier *et al.*, 2004). In the following studies, the concentration-response effects of 67 analogs of MLA on nicotine–stimulated adrenal neurosecretion were investigated (Figure 1) and their IC_{50} values are listed in Table 1. The IC_{50} values of the analogs ranged from 0.9 µM to 115 µM, with a median IC_{50} value of 3.7 µM. In the concentration ranges tested ($\leq$10 µM), these analogs have little or no inhibitory effects on agonist binding to recombinant and native nAChRs, with mean binding effects that are 118.4% ± 2.7% of control, ranging from 69% of control to 174% of control. Only ~4% (3/67) of the analogs at concentrations of 10 µM produced decreases of $\geq$15% in nAChR binding and ~48% (32/67) of the analogs produced apparent increases ($\geq$115% of control) in $\alpha 3\beta 4$ nAChR binding assays at concentrations of 10 µM. For several of the analogs, their direct effects on nAChRs were assessed using cell lines expressing recombinant nAChRs. As can be noted in Tables 3 and 5, the analogs inhibit nicotine-induced increases in free intracellular calcium level with little or no inhibitory effects on agonist binding to nAChRs. These data are consistent with our previous data supporting noncompetitive nAChR inhibition.

All 67 MLA analogs were favorably aligned utilizing GASP-guided sub-group alignment (Figure 2). Subsequent 3D-QSAR analyses were successfully carried out based on this alignment. The statistical significance of the CoMFA model is indicated by

Molecular Pharmacology Fast Forward. Published on February 16, 2007 as DOI: 10.1124/mol.106.033233
This article has not been copyedited and formatted. The final version may differ from this version.

a cross-validated r^2 (q^2) value of 0.648 (Table 2). The model has a correlation of 0.853 (r^2) with electrostatic and steric interactions contributing similarly. The model's predictive power is further corroborated by the predictive r^2 value of 0.904 when applied to an independent test set (Table 2). The alignment of CoMFA fields with the substrate, IB 9, is shown in Figure 3. The IB 9 backbone is covered by yellow contours, which essentially delineates the shape of the receptor binding cavity since these regions represent areas of steric hindrance. The green contour (α) over the phenyl group emphasizes the importance of a sterically bulky group in this binding pocket, likely providing favorable hydrophobic interactions. Similarly, the green contour (β) illustrates the importance of a succinimide group to fill in another binding pocket. The large blue contour (γ) over the ammonium group emphasizes the essential role of a positive charge at this position. The red contour (δ) over the ester carbonyl group and the oxygen atom indicates that negative charges at these positions are favorable for optimum binding.

Based on the same alignment, the CoMSIA model also shows good correlation (r^2 value of 0.906) between hydrophobic, hydrogen-bond acceptor (HBA) interactions and inhibition of neurosecretion. The highly predictive nature of the model is supported by the LOO cross-validation and external test set prediction (q^2 of 0.767 and r^2 of 0.946, respectively, Table 2). When the CoMSIA coefficients are plotted with substrate IB 9 (Figure 4), the large areas surrounding the backbone of IB 9 is covered by yellow contours, which delineate shape requirements of the binding pocket and correlate with unfavorable hydrophobic interactions. The two green contours indicate the important hydrophobic interactions with the phenyl ring (α) and the succinimide group (β). The

Molecular Pharmacology Fast Forward. Published on February 16, 2007 as DOI: 10.1124/mol.106.033233
This article has not been copyedited and formatted. The final version may differ from this version.

blue contour (γ) suggests favorable interactions between amide carbonyl groups (as HBAs) and the binding pocket. The large red contour (δ) suggests the overall preference of less HBA for analog binding.

Table 3 shows the predicted CoMFA and the predicted CoMSIA IC_{50} values, as well as the experimentally-derived functional IC_{50} values for the 6 test set compounds (IB 10, KAB 13, KAB 34, LB 6, PPB 5, and PPB 11). Linear regression analyses of these data (Figure 5) reveal significant correlation ($p<0.05$) between predicted CoMFA and CoMSIA IC_{50} values and experimentally-derived functional IC_{50} values (r^2 values of 0.90 and 0.81, respectively). In addition, the effects of the test set analogs on agonist binding to native and recombinant bovine nAChRs, as well as their effects on the functional activation of native and recombinant nAChRs, are compared. The analogs inhibit activation of recombinant nAChRs and inhibit adrenal neurosecretion at similar concentrations and have little or no inhibitory effects on agonist binding to either native or recombinant nAChRs.

The GASP generated pharmacophore model, based on four structures, contains 10 feature points with an average inter-point distance of 5.43 Å. This machine-generated pharmacophore model was further improved based on knowledge of all 67 compounds and chemical intuition. More specifically, feature points that are specific to a certain structure series as well as duplicate feature points indicating identical pharmacophore features were removed. The resulting, more general, UNITY query contains 3 hydrophobes, 2 HBAs and 1 positively charged nitrogen atom (Figure 6). This knowledge-based pharmacophore model was used to flexibly search two commercially available databases. The resulting hit lists simultaneously served as a

Molecular Pharmacology Fast Forward. Published on February 16, 2007 as DOI: 10.1124/mol.106.033233
This article has not been copyedited and formatted. The final version may differ from this version.

means of model validation and assisted in the selection of molecules for subsequent *in vitro* testing. The data mining yielded multiple hits, eight of which were commercially available compounds. Structures of these compounds are found in Figure 7 and their predicted IC_{50} values are listed in Table 4. None of these compounds inhibited agonist interactions using $\alpha3\beta4$* nAChR binding assays (data not shown). The concentration-response effects of the compounds on adrenal neurosecretion were investigated. Indeed, all proposed compounds inhibited adrenal neurosecretion (Table 4) even though no significant correlations are found when predicted IC_{50} values are plotted versus experimentally-derived IC_{50} values (Figure 8A). This result suggests that when applied to chemical spaces outside that of the training set, our computational model predictions should be interpreted qualitatively (identifying noncompetitive nAChR inhibitors) rather than quantitatively (predicting exact IC_{50} values of these inhibitors).

To further validate the QSAR model, several new MLA analogs were synthesized (Figure 9). COB 1, COB 2, COB 3, and DDR 1 are potent inhibitors of adrenal neurosecretion and also inhibit functional activation of recombinant nAChRs (Table 5). Once again, no inhibition of agonist binding to $\alpha3\beta4$* nAChRs was observed with these compounds. QSAR predictions of their IC_{50} values are comparable to their experimentally-derived functional IC_{50} values (Table 5). Linear regression analyses of these data reveal no significant correlations (Figure 8B). Once again, these data support the qualitative, rather than the quantitative, nature of the model.

Molecular Pharmacology Fast Forward. Published on February 16, 2007 as DOI: 10.1124/mol.106.033233
This article has not been copyedited and formatted. The final version may differ from this version.

DISCUSSION

The principal receptors mediating adrenal neurosecretion are α3β4* nAChRs (Gu *et al.*, 1996; Free *et al.*, 2002; Free *et al.*, 2003), the asterisk indicating the possible presence of additional subunits (Lukas *et al.*, 1999; Free *et al.*, 2003). Our laboratory (Bergmeier *et al.*, 1999; Bryant *et al.*, 2002; Bergmeier *et al.*, 2004), as well as others (Barker *et al.*, 2005), have previously reported the synthesis of several analogs of MLA that appear to act as noncompetitive inhibitors of α3β4* nAChRs. Noncompetitive inhibitors are defined as those compounds that do not compete for binding at the agonist binding site, and yet still bind to the receptor and produce functional effects. In this study, two approaches were used to characterize functional effects of our molecules. Both 1) nicotine-stimulated neurosecretion assays on adrenal chromaffin cells and 2) nicotine-stimulated intracellular calcium measurements using a cell line expressing bovine α3β4 nAChRs were used to identify functional effects of the analogs mediated via native and recombinant nAChRs, respectively. In the second approach, the nicotine-stimulated increase in intracellular calcium is through nAChR-associated ion channels; therefore, inhibition of nicotine-stimulated increases in intracellular free calcium supports a direct action on the analogs on nAChRs. Agonist binding experiments confirm that the analogs are not competitive antagonists. As shown in Table 3, the test set analogs inhibited nicotine-induced increases in intracellular free calcium while having little of no inhibitory effects on agonist binding to recombinant nAChRs. Similar data have been obtained with an additional 30 analogs (data not shown). These data support noncompetitive interactions of the analogs on α3β4 nAChRs.

Molecular Pharmacology Fast Forward. Published on February 16, 2007 as DOI: 10.1124/mol.106.033233
This article has not been copyedited and formatted. The final version may differ from this version.

While most investigations into nAChR drug development have used recombinant nAChRs, these studies have focused on native nAChRs. While there are inherent disadvantages of this approach, one being that the exact subunit composition of the native nAChRs is not known, this approach is likely to yield a better understanding of physiological attributes of the analogs, as well as potential pitfalls in drug design that are not apparent from conventional assays using cells expressing recombinant receptors. These assays involving recombinant nAChRs do not take into account potential analog interactions with other proteins (e.g., additional receptors, ion channels) found in the native environment, leaving out any effects generated by them. Another problem involves the site of action of the analogs or the data-mined molecules. It cannot be established from these studies where these compounds are binding on the receptor protein, and whether they bind to a single site or multiple sites on α3β4* nAChRs. It is well established that multiple noncompetitive binding sites exist on nAChRs (Lloyd and Williams, 2000). One of these sites is located within the nAChR ion channel. This site has been fairly well characterized in muscle nAChRs (Le Novere and Changeux, 1995). Other 'sites' have been described simply as locations at the lipid-protein interface. These studies, also, do not address whether these analogs show nAChR subtype-selectivity or whether the computational models/pharmacophore applies to other nAChR subtypes. Studies involving the localization of the noncompetitive binding site on nAChRs, as well as subtype-specificity of the analogs, are currently in progress.

In these studies the pharmacological activities of 67 MLA analogs were investigated and a putative noncompetitive nAChR recognition site and a noncompetitive pharmacophore are proposed. Few studies have had such wealth of

Molecular Pharmacology Fast Forward. Published on February 16, 2007 as DOI: 10.1124/mol.106.033233
This article has not been copyedited and formatted. The final version may differ from this version.

structurally similar compounds for analyses. We have found that the more potent of these MLA analogs have functional IC_{50} values in the low micromolar range, similar to potencies of other antagonists of adrenal neurosecretion including hexamethonium, decamethonium, d-tubocurarine, tetracaine, pentolinium, and mecamylamine (IC_{50} values ranging for 17 to 0.1 μM) (McKay and Sanchez, 1990; McKay and Burkman, 1993). In addition, two classic noncompetitive inhibitors of muscle nAChRs, phencyclidine (PCP) and histrionicotoxin (HTX), and have affinities in the micromolar and submicromolar range (~1 μM and ~ 0.3 μM, respectively) (Heidmann *et al.*, 1983). Through structural modification of our compounds, we have increased potencies of these compounds into ranges that currently exist for noncompetitive nAChR antagonists, supporting the use of MLA analogs to elucidate structural determinants important for nAChR activity.

The conventional target for drug development has been the agonist binding site of nAChRs, located on α nAChR subunits. Not unexpectedly, the binding sites on different α subunits have a high degree of amino acid similarity. From an evolutionary perspective, selective pressure has forced this similarity due to interaction of these sites with the endogenous neurotransmitter, acetylcholine. The lack of pharmacologically specific agonists and antagonists directed at these sites is likely related to the physiochemical resemblance of agonist binding sites. The selectivity of most agonists and competitive antagonists is modest, at best. As a novel approach for neuronal nAChR drug discovery, our laboratory has targeted other ‘sites’ (noncompetitive sites, negative allosteric binding sites) located on nAChRs. Similar approaches were used on

Molecular Pharmacology Fast Forward. Published on February 16, 2007 as DOI: 10.1124/mol.106.033233
This article has not been copyedited and formatted. The final version may differ from this version.

$GABA_A$ receptors (Olsen *et al.*, 2004) and the discovery of the benzodiazepine binding site has led to an important therapeutic class of drugs.

Pharmacophore development for noncompetitive nAChR binding sites is hampered by a lack of specific, high affinity, radiolabeled ligands. The availability of native cells expressing neuronal nicotinic receptors, functional assays for studies on the pharmacological effects of molecules, and a large number of structurally-related molecules, presented a unique opportunity for the development of a pharmacophore model for noncompetitive binding sites. Indeed, two 3D-QSAR models and one pharmacophore model were successfully generated based on these data. The CoMFA model explained the binding affinity using steric and electrostatic interactions while the CoMSIA model correlated the same activity with hydrophobic and HBA interactions. Both the CoMFA and CoMSIA models clearly delineated the binding pocket. Additionally, the CoMFA model identified the positive charge provided by the amine group and the negative charge carried by the ester carbonyl group as essential for binding. The CoMSIA model emphasized the important role of the amide carbonyl group from the succinimide ring as an HBA needed in docking to the binding site. Both models were highly predictive in calculating an external test set. They also successfully categorized the retrieved compounds from pharmacophore-based database screening.

With three HYPs (hydrophobic features), two HBAs and one positive charged nitrogen atom, the pharmacophore prototype echoes the findings of 3D-QSAR models and provides more direct visualization of binding requirements (Figure 6). The prospective application of this pharmacophore model in screening two commercial molecule databases (Chembridge and Spec) successfully retrieved several molecules

Molecular Pharmacology Fast Forward. Published on February 16, 2007 as DOI: 10.1124/mol.106.033233
This article has not been copyedited and formatted. The final version may differ from this version.

with relatively high potency in our functional assays. The data found in Tables 4 and 5, showing the qualitative agreement between the model-derived IC_{50} values and experimentally-derived functional IC_{50} values, support the predictive nature of our computational models as seen by the abilities of the pharmacophore model to retrieve promising molecules and the 3D-QSAR model to confirm inhibitory activity. The ability of the computational models to rapidly identify novel ligands should contribute significantly to drug development in this area.

The studies described here represent the first attempt to define a novel pharmacophore on α3β4* nAChRs using a large number of MLA analogs. The physiochemical characterization of these noncompetitive binding sites on α3β4* nAChRs should improve our understanding of the composition and functioning of nAChRs. As these studies demonstrate, application of the pharmacophore model in database mining led to the rapid identification of with pharmacological activity. These data support the utility of the computational models as tools for the efficient retrieval of novel nAChR inhibitors that may lead to the identification of new therapeutic drugs that target novel sites on nAChRs.

Molecular Pharmacology Fast Forward. Published on February 16, 2007 as DOI: 10.1124/mol.106.033233
This article has not been copyedited and formatted. The final version may differ from this version.

REFERENCES

Barker D, Lin DHS, Carland JE, Chu CPY, Chebib M, Brimble MA, Savage GP and McLeod MD (2005) Methyllycaconitine analogues have mixed antagonist effects at nicotinic acetylcholine receptors. *Bioorg Med Chem* 13:4565-4575.

Bergmeier SC, Ismail KA, Arason KM, McKay S, Bryant DL and McKay DB (2004) Structure activity studies of ring E analogues of methyllycaconitine. Part 2: synthesis of antagonists to the α3β4 nicotinic acetylcholine receptors through modifications to the ester. *Bioorg Med Chem Lett* 14:3739-3742.

Bergmeier SC, Lapinsky DJ, Free RB and McKay DB (1999) Ring E analogs of methyllycaconitine (MLA) as novel nicotinic antagonists. *Bioorg Med Chem Lett* 9:2263-2266.

Bohacek RS and McMartin C (1992) Definition and display of steric, hydrophobic, and hydrogen-bonding properties of ligand binding sites in proteins using Lee and Richards accessible surface: validation of a high-resolution graphical tool for drug design. *J Med Chem* 35:1671-1684.

Bryant DL, Free RB, Thomasy SM, Lapinsky DJ, Ismail KA, McKay SB, Bergmeier SC and McKay DB (2002) Structure-activity studies with ring E analogues of methyllycaconitine on bovine adrenal α3β4* nicotinic receptors. *Neurosci Res* 42:57-63.

Clark M and Cramer III RD (1993) The probability of chance correlation using partial least squares (PLS). *Quant Struct -Act Relat* 12:137-145.

Cramer RD, Patterson DE and Bunce JD (1988) Comparative molecular field analysis (CoMFA). 1. Effect of shape on binding of steroids to carrier proteins. *J Am Chem Soc* 110:5959-5967.

Daly JW (2005) Nicotinic agonists, antagonists, and modulators from natural sources. *Cell Mol Neurobiol* 25:513-552.

Free RB, Bryant DL, McKay SB, Kaser DJ and McKay DB (2002) [^{3}H]Epibatidine binding to bovine adrenal medulla: evidence for $\alpha3\beta4$* nicotinic receptors. *Neurosci Lett* 318:98-102.

Free RB, von Fischer ND, Boyd RT and McKay DB (2003) Pharmacological characterization of recombinant bovine $\alpha3\beta4$ neuronal nicotinic receptors stably expressed in HEK 293 cells. *Neurosci Lett* 343:180-184.

Goodall K, Barker D and Brimble MA (2005) A review of advances in the synthesis of analogues of the *delphenium* alkaloid methyllycaconitine. *Synlett* 12:1809-1827.

Gu H, Wenger BW, Lopez I, McKay SB, Boyd RT and McKay DB (1996) Characterization and localization of adrenal nicotinic receptors: evidence that mAb35-nicotinic receptors are the principal receptors mediating adrenal catecholamine secretion. *J Neurochem* 66:1454-1461.

Heidmann T, Oswald RE and Changeux JP (1983) Multiple sites of action for noncompetitive blockers on acetylcholine receptor rich membrane fragments from torpedo marmorata. *Biochem* 22:3112-3127.

Hurst T (1994) Flexible 3D searching: The directed tweak technique. *J Chem Inf Comput Sci* 34:190-196.

Jones G, Willett P and Glen RC (1995) A genetic algorithm for flexible molecular overlay and pharmacophore elucidation. *J Comput Aided Mol Des* 9:532-549.

Klebe G, Abraham U and Mietzner T (1994) Molecular similarity indices in a comparative analysis (CoMSIA) of drug molecules to correlate and predict their biological activity. *J Med Chem* 37:4130-4146.

Kroemer RT and Hecht P (1995) Replacement of steric 6-12 potential-derived interactions energies by atom-based indicator variables in CoMFA leads to models of higher consitency. *J Comput Aided Mol Des* 9:205-212.

Le Novere N and Changeux JP (1995) Molecular evolution of the nicotinic acetylcholine receptor: an example of multigene family in excitable cells. *J Mol Evol* 40:155-172.

Livett BG, Gayler KR and Khalil Z (2004) Drugs from the sea: conopeptides as potential therapeutics. *Curr Med Chem* 11:1715-1723.

Lloyd GK and Williams M (2000) Neuronal nicotinic acetylcholine receptors as novel drug targets. *J Pharmacol Exp Ther* 292:461-467.

Luetje CW, Wada K, Rogers S, Abramson SN, Tsuji K, Heinemann S and Patrick J (1990) Neurotoxins distinguish between different neuronal nicotinic acetylcholine receptor subunit combinations. *J Neurochem* 55:632-640.

Lukas RJ, Changeux J-P, le Novère N, Albuquerque EX, Balfour JK, Berg DK, Bertrand D, Chiappinelli VA, Clarke PBS, Collins AC, Dani JA, Grady SR, Kellar KJ, Lindstrom JM, Marks MJ, Quik M, Taylor PW and Wonnacott S (1999) International union of pharmacology. XX. Current status of the nomenclature for nicotinic acetylcholine receptors and their subunits. *Pharmacol Rev* 51:397-401.

Maurer JA and McKay DB (1994) Staurosporine-induced reduction of secretory function in cultured bovine adrenal chromaffin cells. *Eur J Pharmacol* 253:115-124.

McKay DB and Burkman AM (1993) Nicotinic and non-nicotinic receptor-mediated actions of vinblastine. *Proc Soc Exp Biol Med* 203:372-376.

McKay DB and Sanchez AP (1990) Effect of noncompetitive nicotinic receptor blockers on catecholamine release from cultured adrenal chromaffin cells. *Pharmacology* 40:224-230.

Olsen RW, Chang CS, Li G, Hanchar HJ and Wallner M (2004) Fishing for allosteric sites on $GABA_A$ receptors. *Biochem Pharmacol* 68:1675-1684.

Ward JM, Cockcroft VB, Lunt GG, Smillie FS and Wonnacott S (1990) Methyllycaconitine: a selective probe for neuronal α-bungarotoxin binding sites. *FEBS Lett* 270:45-48.

Xiao Y, Meyer EL, Thompson JM, Surin A, Wroblewski J and Kellar KJ (1998) Rat α3/β4 subtype of neuronal nicotinic acetylcholine receptor stably expressed in a transfected cell line: pharmacology of ligand binding and function. *Mol Pharmacol* 54:322-333.

Yum L, Wolf KM and Chiappinelli VA (1996) Nicotinic acetylcholine receptors in separate brain regions exhibit different affinities for methyllycaconitine. *Neurosci* 72:545-555.

Molecular Pharmacology Fast Forward. Published on February 16, 2007 as DOI: 10.1124/mol.106.033233
This article has not been copyedited and formatted. The final version may differ from this version.

FOOTNOTES

This project was supported by NIH Grants DA12707 (SCB, DBM) and DA10569 (DBM). DLB was supported as a NIDA Underrepresented Minority Supplement Awardee (DA10569).

Reprint Requests: Dennis B. McKay, Ph.D.

Division of Pharmacology

The Ohio State University

College of Pharmacy

500 West 12th Avenue

Columbus, Ohio 43210

email: mckay.2@osu.edu

Molecular Pharmacology Fast Forward. Published on February 16, 2007 as DOI: 10.1124/mol.106.033233
This article has not been copyedited and formatted. The final version may differ from this version.

LEGENDS FOR FIGURES

FIGURE 1. Structures of compounds listed in Tables 1 and 3.

FIGURE 2. Overall alignment of all 67 compounds used in generating the following 3D-QSAR models. All 67 structures are shown as wireframe representation.

FIGURE 3. CoMFA model of analog binding. CoMFA coefficient contours map aligned with inhibitor IB 9. The contours of the steric map are shown in yellow and green, while the contours of the electrostatic map are shown in red and blue. Greater antagonism (lower IC_{50} values) is correlated with less bulk near yellow (17%), more bulk near green (20%), more negative charge near red (20%), and more positive charge near blue (20%).

FIGURE 4. CoMSIA model of pharmacophore. CoMSIA contours aligned with inhibitor IB 9. The contours of the hydrophobic map are shown in yellow and green, while the contours of the HBA map are shown in red and blue. Greater inhibition (lower IC_{50} values) is correlated with less bulk near yellow (18%), more bulk near green (20%), more HBA near blue (20%), and less HBA near red (20%).

FIGURE 5. Linear regression analyses of predicted and experimentally-derived functional IC_{50} values of test set compounds. Predicted and experimentally-derived functional IC_{50} values of test set compound (IB 10, KAB 13, KAB 34, LB 6, PPB 5, and

PPB11) using CoMFA model (A) or CoMSIA model (B). IC_{50} values of test set compounds are listed in Table 1.

FIGURE 6. Pharmacophore model generated using GASP. The pharmacophore features are illustrated using IB 9. HYD, hydrophobic feature; HBA, hydrogen bond acceptor feature; PosN, positive charged nitrogen feature.

FIGURE 7. Structures of compounds listed in Table 4.

FIGURE 8. Comparison of predicted and experimentally-derived functional IC_{50} values. (A) Predicted and experimentally-derived functional IC_{50} values of (A) compounds obtained from data mining and (B) new MLA analogs not used in pharmacophore modeling. Predicted and experimentally-derived IC_{50} values are found in Table 4 (A) and Table 5 (B).

FIGURE 9. Structures of compounds listed in Table 5.

Molecular Pharmacology Fast Forward. Published on February 16, 2007 as DOI: 10.1124/mol.106.033233
This article has not been copyedited and formatted. The final version may differ from this version.

TABLE 1. Effects of analogs on adrenal neurosecretion

Analog	Nicotine-Stimulated Neurosecretion (IC_{50}, μM)[a]	Analog	Nicotine-Stimulated Neurosecretion (IC_{50}, μM)[a]	Analog	Nicotine-Stimulated Neurosecretion (IC_{50}, μM)[a]
Figure 1A Analogs		**Figure 1B Analogs**		**Figure 1C Analogs**	
KAB 37	1.9 (1.6-2.2)	**PPB 13**	0.9 (0.8-1.1)	**PPB 3**	1.0 (0.9-1.2)
KAB 36	2.0 (1.8-2.2)	**KAB 20**	1.3 (1.2-1.6)[c]	**PPB 5**[d]	1.2 (1.1-1.3)
KAB 14	2.1 (1.9-2.4)	**KAB 18**	1.7 (1.6-1.8)[c]	**PPB 7**	1.2 (1.1-1.3)
KAB 16	2.5 (2.3-2.8)	**KAB 21**	3.0 (2.3-3.9)[c]	**IB 12**	1.2 (1.2-1.3)
KAB 17	2.7 (2.3-3.1)	**KAB 23**	3.2 (3.1-3.4)[c]	**IB 10**[d]	1.3 (1.1-1.4)[c]
KAB 11	2.8 (2.4-3.1)	**KAB 24**	3.2 (3.1-3.2)[c]	**IB 11**	1.3 (0.7-2.4)[c]
KAB 35	3.3 (2.8-3.9)	**KAB 22**	3.4 (3.2-3.5)[c]	**JHB 1**	1.3 (1.1-1.5)
KAB 10	3.5 (3.5-3.6)	**KAB 25**	5.2 (4.8-5.6)[c]	**PPB 4**	1.3 (1.2-1.3)
KAB 38	3.5 (3.2-3.8)	**KAB 31**	6.0 (5.5-6.6)[c]	**IB 8**	1.5 (1.5-1.5)[c]
KAB 12	3.7 (3.4-3.9)	**KAB 30**	7.5 (6.8-7.6)[c]	**PPB 6**	1.6 (1.6-1.7)
KAB 33	4.2 (3.6-4.9)	**KAB 19**	8.4 (7.8-9.1)[c]	**PPB 1**	1.7 (1.5-1.9)
KAB 13[d]	4.4 (4.3-4.6)	**Figure 1D Analogs**		**IB 9**	1.7 (1.7-1.7)[c]
KAB 15	4.6 (4.0-5.3)	**APB 3**	2.1 (1.5-2.8)	**IB 7**	2.5 (2.3-2.6)[c]
KAB 29	5.3 (5.0-5.5)	**APB 2**	2.8 (2.5-3.1)	**PPB 11**[d]	2.6 (2.2-3.1)
KAB 8	5.4 (5.0-5.8)	**APB 8**	2.8 (2.1-3.9)	**IB 6**	4.0 (3.7-4.3)[c]
KAB 34[d]	6.2 (5.3-7.2)	**APB 9**	4.0 (3.2-4.8)	**PPB 10**	4.1 (3.8-4.5)
KAB 32	6.7 (6.0-7.5)	**APB 6**	6.6 (6.1-7.2)	**PPB 9**	5.7 (5.0-6.5)
KAB 9	6.9 (6.5-7.3)	**APB 5**	7.1 (5.8-8.7)	**LB 5**	65 (53-80)[b]
LB 8	11 (10-12)[b]	**APB 10**	8.2 (6.2-9.8)	**LB 4**	114 (96-138)[b]
IB 1	20 (19-21)[b]	**APB 4**	$\geq$10	**Figure 1E Analogs**	
AB 2	27 (24-32)	**APB 1**	$\geq$10	**APB 12**	13.0 (11-16)
LB 3	37 (28-48)[b]			**APB 11**	$\geq$10
LB 7	52 (48-57)[b]				
LB 6[d]	59 (55-63)[b]				
LB 1	63 (55-73)[b]				
LB 2	62 (59-66)[b]				

[a] Concentration–response effects of the analogs were determined as described in the methods section; IC_{50} values represent geometric means (confidence limits), n=3-7.
[b] Data are from Bryant et al. (Bryant *et al.*, 2002).
[c] Data from Bergmeier et al. (Bergmeier *et al.*, 2004).
[d] Test set compounds.

Molecular Pharmacology Fast Forward. Published on February 16, 2007 as DOI: 10.1124/mol.106.033233
This article has not been copyedited and formatted. The final version may differ from this version.

TABLE 2. Statistics for CoMFA and CoMSIA models.

	q^2	Press	n	r^2	S	%Steric	%Electrostatic	$^{c}q^2$
CoMFA	0.648	0.301	3	0.853	0.194	53	47	0.904
CoMSIA	0.767	0.247	4	0.906	0.16	75[a]	25[b]	0.946

[a] % Hydrophobic interaction
[b] % H-bond acceptor interaction
[c] test set prediction

TABLE 3. Comparison of predicted and experimentally-derived IC_{50} values of test set compounds.

			Native nAChRs	Recombinant nAChRs	Native nAChRs	Recombinant nAChRs
	CoMFA	CoMSIA	Nicotine-Stimulated Neurosecretion[a]	Nicotine-Stimulated $[Ca^{2+}]_i$[b]	nAChR Binding[c]	nAChR Binding[c]
Analog	IC_{50} Values (μM)	IC_{50} Values (μM)	IC_{50} Values (μM)	IC_{50} Values (μM)	Specific Binding (% Control)	Specific Binding (% Control)
IB 10	1.2	1.3	1.3 (1.1-1.4)	7.6 (6.8-8.6)	151.3 ± 15.7	99.6 ± 0.4
KAB 13	7.2	4.0	4.4 (4.3-4.6)	ND	114.3 ± 1.4	95.0 ± 0.9
KAB 34	2.8	3.0	6.2 (5.3-7.2)	3.1 (2.8-3.5)	83.2 ± 1.4	88.2 ± 11.6
LB 6	40.7	47.9	59.6 (55.6-63.9)	ND	92.4 ± 4.9[d]	ND
PPB 5	1.5	1.6	1.2 (1.1-1.3)	13.4 (10.3-17.3)	152.8 ± 7.6	90.8 ± 1.6
PPB 11	1.4	1.9	2.6 (2.2-3.1)	8.0 (5.9-10.8)	118.4 ± 12.5	99.9 ± 12.3

[a] Data are from Table 1

[b] Inhibition curves were generated as described in the methods section; values represent geometric means (confidence limits), n=4

[c] Competition binding experiments were performed at a fixed concentration of each analog (10μM), as described in the methods section; values represent arithmetic means ± SEM, n=3-7.

[d] Competition binding experiments were performed at a fixed antagonist concentration of 100μM.

Molecular Pharmacology Fast Forward. Published on February 16, 2007 as DOI: 10.1124/mol.106.033233
This article has not been copyedited and formatted. The final version may differ from this version.

TABLE 4. Comparison of predicted and experimentally-derived IC_{50} values from hit compounds returned from database screening.

Compound	Predicted IC_{50} Values (μM)[a]	Experimentally-derived Neurosecretion IC_{50} Values (μM)[b]
Chembridge 60481	5.0	9.7 (6.9 -12)
Chembridge 61053	17.2	7.7 (6.7-8.8)
Chembridge 80200	14.7	6.1 (4.9-7.6)
Spec 151790	29.5	7.4 (6.5-8.5)
Spec 147624	7.9	49.5 (24.7-99.5)
Spec 201662	11.8	15 (11.9-19.0)
Spec 201708	9.9	12.4 (11.5-13.4)
Spec 190968	25.6	33.9 (31.6-36.3)

[a] Predicted IC_{50} values were calculated using CoMFA model
[b] Functional inhibition curves were generated as described in the methods section; values represent geometric means (confidence limits), n=3-5.

Molecular Pharmacology Fast Forward. Published on February 16, 2007 as DOI: 10.1124/mol.106.033233
This article has not been copyedited and formatted. The final version may differ from this version.

TABLE 5. Comparison of predicted and experimentally-derived IC_{50} values of MLA analogs

Analog		Native nAChRs	Recombinant nAChRs	Native nAChRs
	CoMFA Prediction	Nicotine-Stimulated Neurosecretion	Nicotine-Stimulated $[Ca^{2+}]_i$	
	IC_{50} Values (μM)[a]	IC_{50} Values (μM)[b]	IC_{50} Values (μM)[b]	Specific Binding (% Control)[c]
COB 1	2.7	3.5 (3.1-3.9)	1.2 (1.0-1.4)	113.5% ± 4.8%
COB 2	9.8	1.2 (1.2-1.3)	1.1 (1.0-1.1)	125.8% ± 3.8%
COB 3	6.1	3.0 (2.5-3.7)	0.7 (0.6-0.9)	106.0% ± 2.5%
DDR 1	11.5	1.7 (1.4-2.0)	30.0 (23.5-38.3)	118.7% ± 13.9%

[a] Predicted IC_{50} values were calculated using CoMFA model
[b] Inhibition curves were generated as described in the methods section; values represent geometric means (confidence limits), n=4-6
[c] Competition binding experiments were performed with a fixed concentration of each analog (10μM), as described in the methods section; values represent arithmetic means ± SEM, n=4.

Molecular Pharmacology Fast Forward. Published on February 16, 2007 as DOI: 10.1124/mol.106.033233
This article has not been copyedited and formatted. The final version may differ from this version.

Figure 1

A

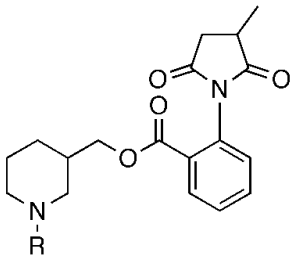

R = $(CH_2)_3CH_3$, **AB-2**
R = $(CH_2)_3$-cC_6H_{11}, **KAB-8**
R = $(CH_2)_5Ph$, **KAB-10**
R = $(CH_2)_6Ph$, **KAB-11**
R = $(CH_2)_4Ph$, **KAB-29**
R = CH_3, **LB-1**
R = CH_2CH_3, **LB-2**
R = $CH(CH_3)_2$, **LB-3**
R = $(CH_2)_2OCH_2CH_3$, **LB-6**
R = $(CH_2)_2Ph$, **LB-7**
R = $(CH_2)_3Ph$, **LB-8**
R = $(CH_2)_2OPh$, **IB-1**

n = 2, Ar = 4-OCH_3-Ph, **KAB-9**
n = 2, Ar = 4-Cl-Ph, **KAB-12**
n = 2, Ar = 4-CH_3-Ph, **KAB-13**
n = 2, Ar = 3,4-Cl_2-Ph, **KAB-14**
n = 2, Ar = 3-Cl-Ph, **KAB-15**
n = 2, Ar = 1-naphthyl, **KAB-16**
n = 2, Ar = 2-naphthyl, **KAB-17**
n = 4, Ar = Ph, **KAB-32**
n = 5, Ar = Ph, **KAB-33**
n = 4, Ar = 4-OCH_3-Ph, **KAB-34**
n = 5, Ar = 4-OCH_3-Ph, **KAB-35**
n = 2, Ar = 3-CF_3, 4-Cl-Ph, **KAB-36**
n = 4, Ar = 3,4-Cl_2-Ph, **KAB-37**
n = 5, Ar = 3,4-Cl_3-Ph, **KAB-38**

B

X = Ph, Y = H, **KAB-18**
X = NHAc, Y = H, **KAB-19**
X = phenylsuccinimide, Y = H, **KAB-20**
X = H, Y = Ph, **KAB-21**
X = Cl, Y = H, **KAB-22**
X = OCH_3, Y = H, **KAB-23**
X = CF_3, Y = H, **KAB-24**
X = F, Y = H, **KAB-25**
X = 3,3-dimethylsuccinimide, Y = H, **KAB-30**
X = 3,4-dimethylsuccinimide, Y = H, **KAB-31**
X = Ph, Y = H, **PPB-13** (*R*-enantiomer)

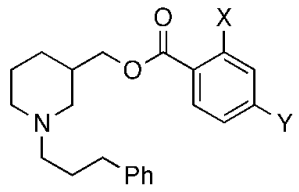

C

R = $CH(CH_3)_2$, R' = H, **LB-4**
R = $(CH_2)_3CH_3$, R' = H, **LB-5**
R = $(CH_2)_3Ph$, R' = CH_2CH_3, **IB-6**
R = $(CH_2)_3Ph$, R' = $CH(CH_3)_2$, **IB-7**
R = $(CH_2)_3Ph$, R' = $(CH_2)_3CH_3$, **IB-8**
R = $(CH_2)_3Ph$, R' = CH_2CHCH_2, **IB-9**
R = $(CH_2)_3Ph$, R' = CH_2Ph, **IB-10**
R = $(CH_2)_3Ph$, R' = $(CH_2)_7CH_3$, **IB-11**
R = $(CH_2)_3Ph$, R' = cC_5H_9, **IB-12**
R = $(CH_2)_3Ph$, R' = CH_2(4-Cl-Ph), **PPB-1**
R = $(CH_2)_3Ph$, R' = $(CH_2)_2Ph$, **PPB-3**
R = $(CH_2)_3Ph$, R' = $(CH_2)_2CHCH_2$, **PPB-4**
R = $(CH_2)_3Ph$, R' = CH_2(4-OCH_3-Ph), **PPB-5**
R = $CH(CH_3)_2$, R' = CH_2Ph, **PPB-6**
R = CH_2-cC_6H_{11}, R' = CH_2Ph, **PPB-7**
R = CH_2CH_3, R' = CH_2Ph, **PPB-9**
R = CH_2CHCH_2, R' = CH_2Ph, **PPB-10**
R = $(CH_2)_2Ph$, R' = CH_2Ph, **PPB-11**
R = $(CH_2)_4O$(3,4-Cl_2-Ph), R' = CH_2Ph, **JHB-1**

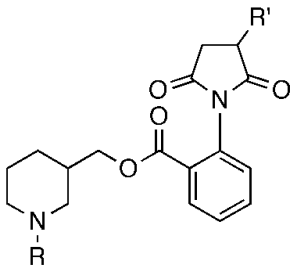

D

R = $(CH_2)_5O$(4-OCH_3-Ph), Ar = 2-chromone, **APB-1**
R = $(CH_2)_5O$(4-OCH_3-Ph), Ar = 4-Ph-Ph, **APB-2**
R = $(CH_2)_5O$(4-OCH_3-Ph), Ar = 3-coumarin, **APB-3**
R = $(CH_2)_5O$(4-Cl-Ph), Ar = 2-Ph-Ph, **APB-4**
R = $(CH_2)_5O$(4-Cl-Ph), Ar = 4-Ph-Ph, **APB-5**
R = $(CH_2)_5O$(4-Cl-Ph), Ar = 3-chromone, **APB-6**
R = $(CH_2)_5O$(4-OCH_3-Ph), Ar = 2-Ph-Ph, **APB-8**
R = $(CH_2)_5O$(4-Cl-Ph), Ar = 3-coumarin, **APB-9**
R = $(CH_2)_5O$(4-OCH_3-Ph), Ar = 3-chromone, **APB-10**

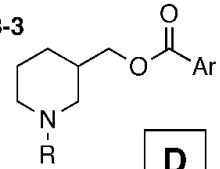

E

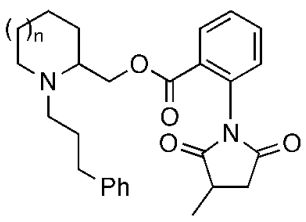

n = 1, **APB-11**
n = 0, **APB-12**

Molecular Pharmacology Fast Forward. Published on February 16, 2007 as DOI: 10.1124/mol.106.033233
This article has not been copyedited and formatted. The final version may differ from this version.

Figure 2

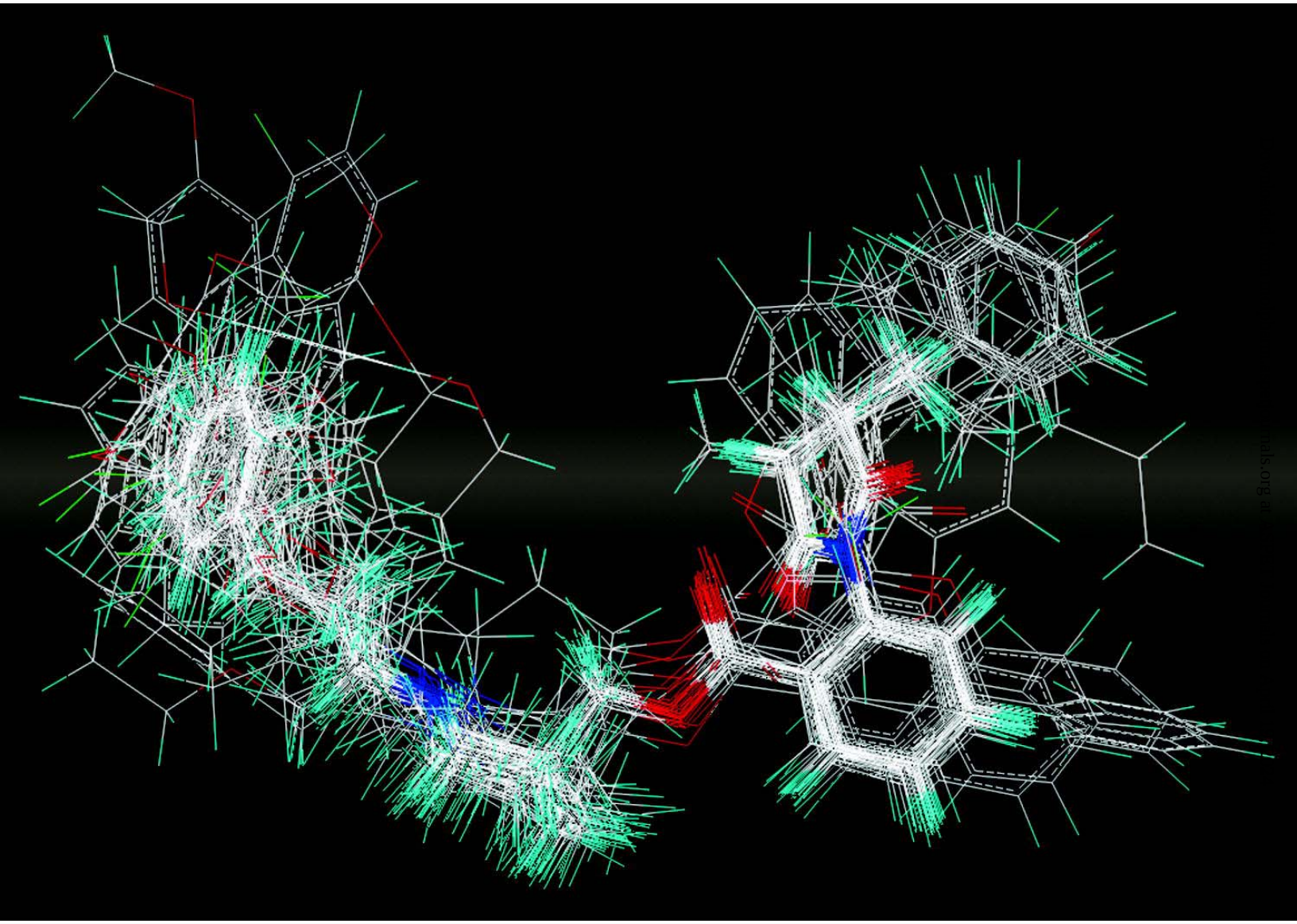

Molecular Pharmacology Fast Forward. Published on February 16, 2007 as DOI: 10.1124/mol.106.033233
This article has not been copyedited and formatted. The final version may differ from this version.

Figure 3

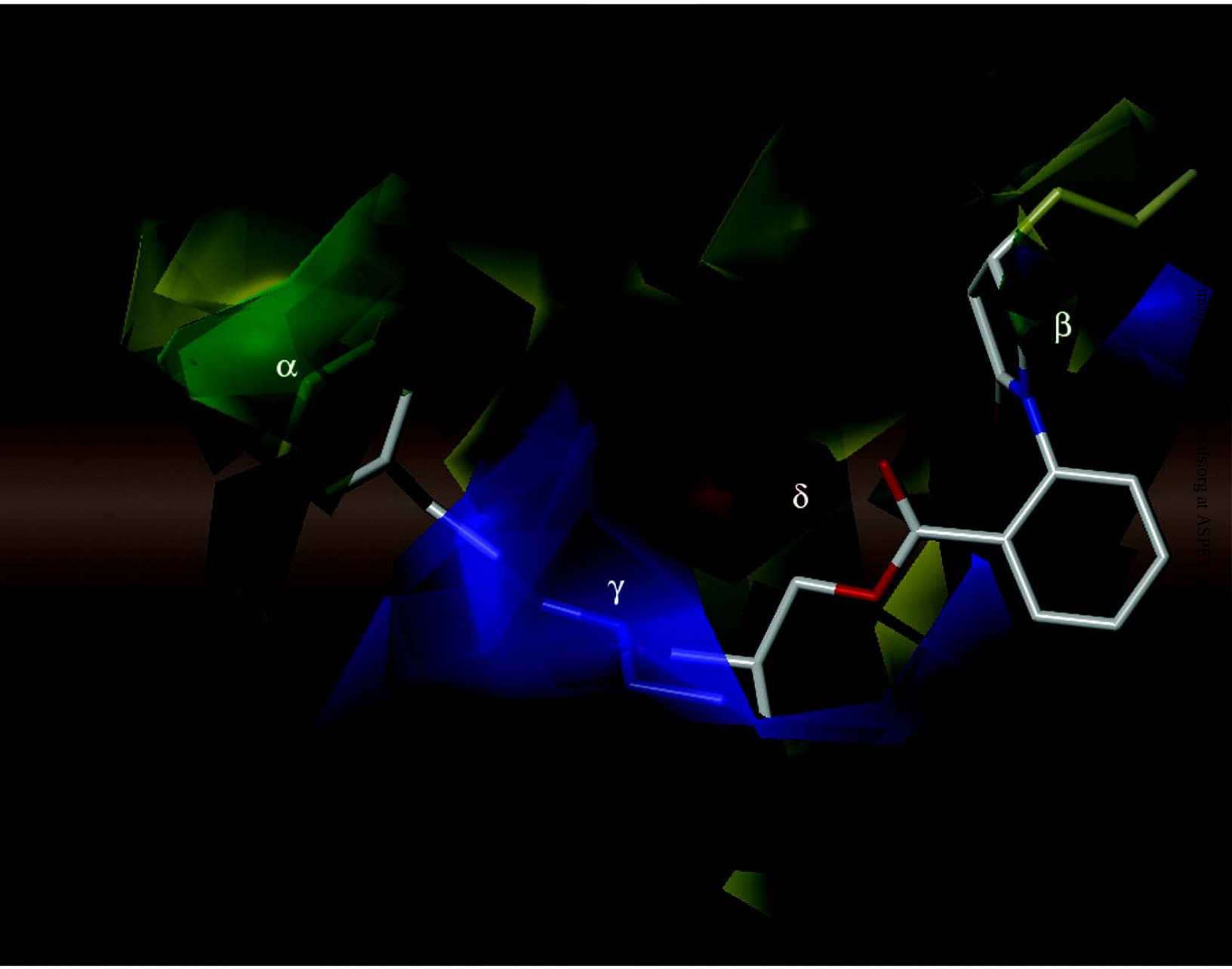

Molecular Pharmacology Fast Forward. Published on February 16, 2007 as DOI: 10.1124/mol.106.033233
This article has not been copyedited and formatted. The final version may differ from this version.

Figure 4

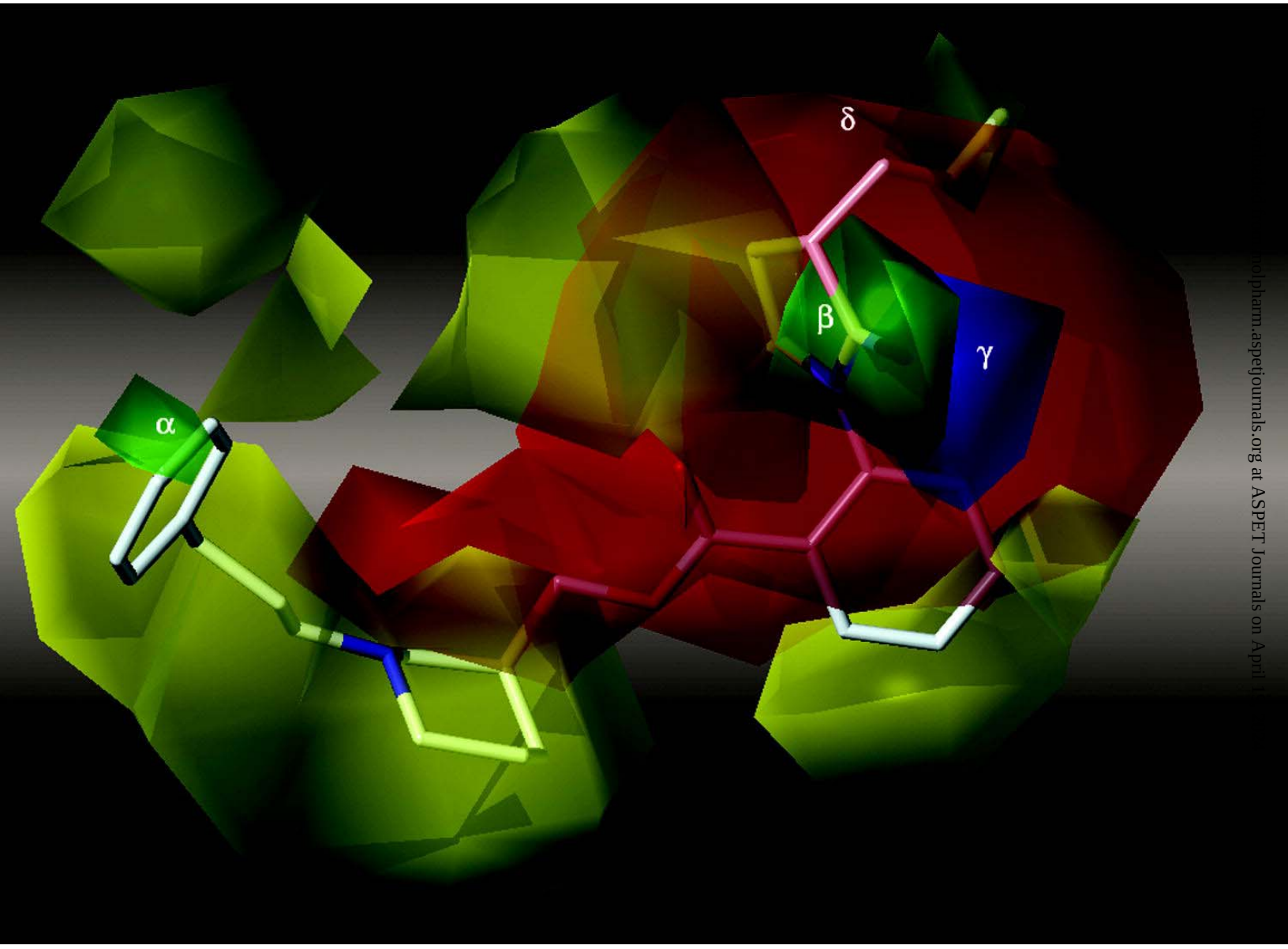

Molecular Pharmacology Fast Forward. Published on February 16, 2007 as DOI: 10.1124/mol.106.033233
This article has not been copyedited and formatted. The final version may differ from this version.

Figure 5

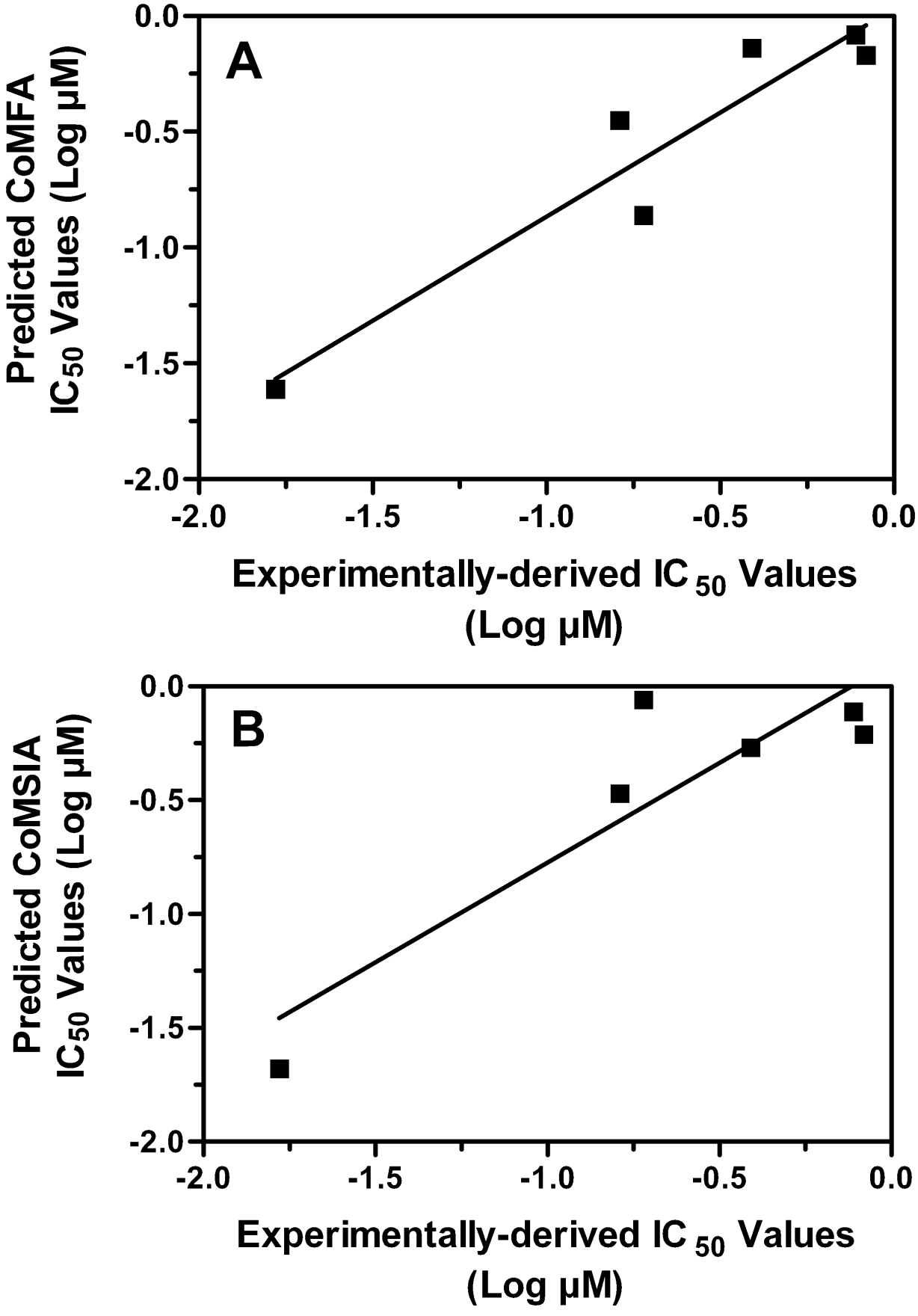

Molecular Pharmacology Fast Forward. Published on February 16, 2007 as DOI: 10.1124/mol.106.033233
This article has not been copyedited and formatted. The final version may differ from this version.

Figure 6

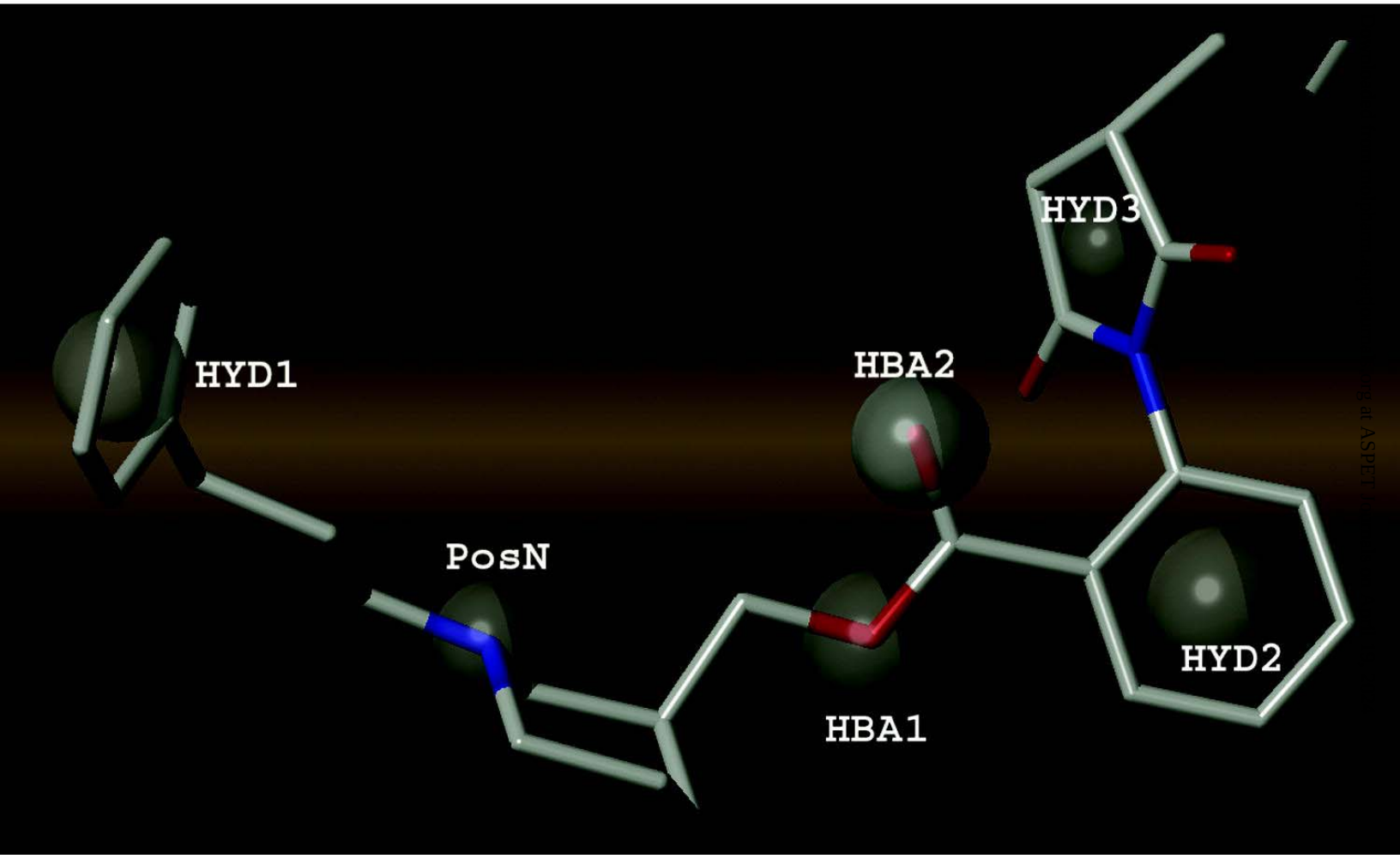

Molecular Pharmacology Fast Forward. Published on February 16, 2007 as DOI: 10.1124/mol.106.033233
This article has not been copyedited and formatted. The final version may differ from this version.

Figure 7

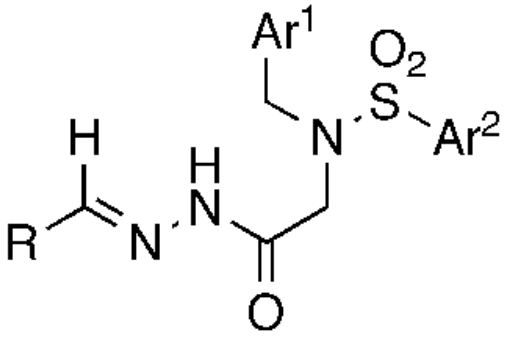

R = 3-(Oallyl)Ph, Ar^1 = Ph, Ar^2 = Ph, **Chembridge-60481**
R = 4-(Oallyl)Ph, Ar1 = Ph, Ar^2 = Ph, **Chembridge-61053**
R = $(CH_2)_2$Ph, Ar^1 = 2-furyl, Ar^2 = Ph, **Chembridge-80200**
R = 3-(Oallyl)Ph, Ar^1 = Ph, Ar^2 = 2,5-Cl_2-Ph, **Spec-201662**
R = 3-(Oallyl)Ph, Ar^1 = 4-Br-Ph, Ar^2 = Ph, **Spec-201708**
R = 3,4-$(OEt)_2$-Ph, Ar^1 = 2-Cl-Ph, Ar^2 = 4-Cl-Ph, **Spec-190968**

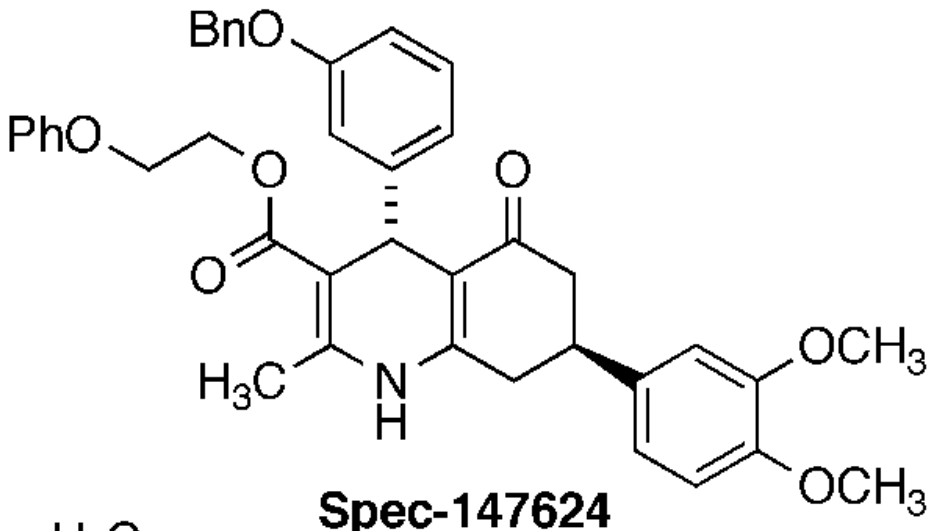

Spec-147624

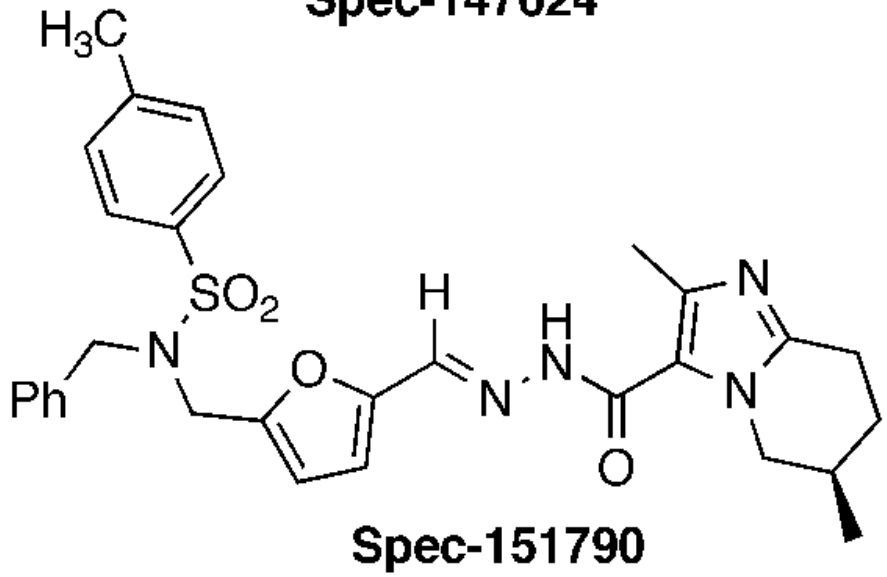

Spec-151790

Molecular Pharmacology Fast Forward. Published on February 16, 2007 as DOI: 10.1124/mol.106.033233
This article has not been copyedited and formatted. The final version may differ from this version.

Figure 8

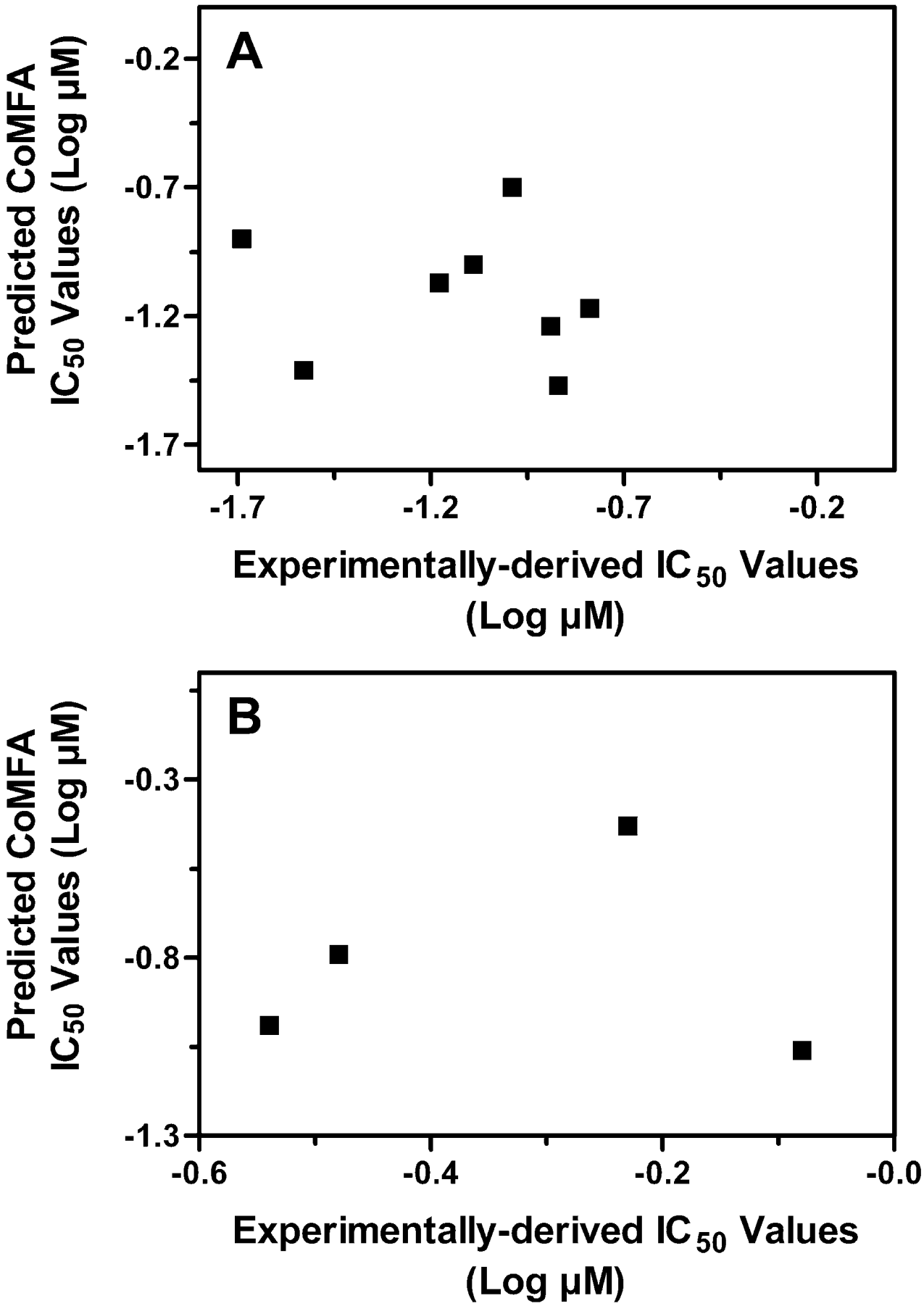

Molecular Pharmacology Fast Forward. Published on February 16, 2007 as DOI: 10.1124/mol.106.033233
This article has not been copyedited and formatted. The final version may differ from this version.

Figure 9

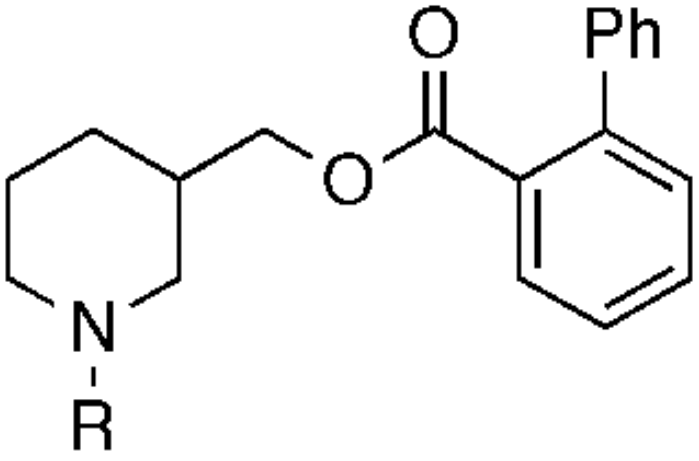

R = H, **COB-1**
R = CH_3, **COB-2**

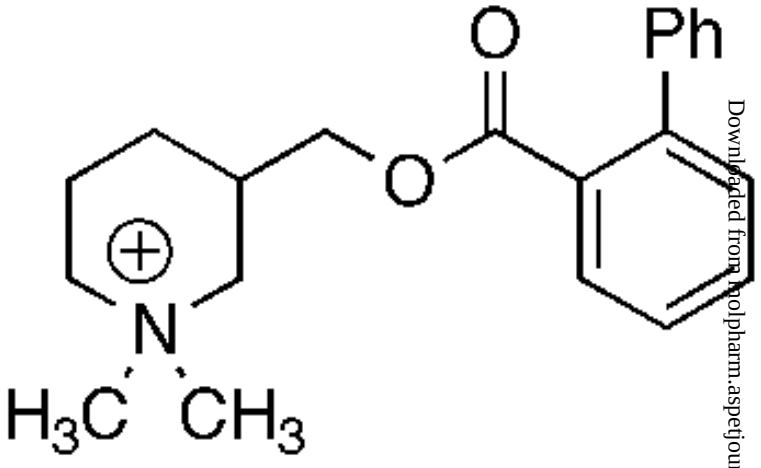

COB-3

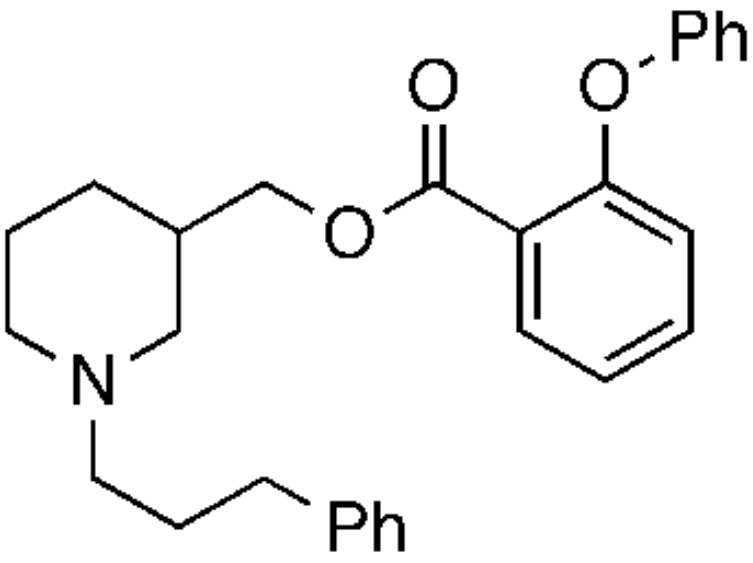

DDR-1